Coordinated Incorporation of Skeletal Muscle Dihydropyridine Receptors and Ryanodine Receptors in Peripheral Couplings of BC_3H1 Cells

Feliciano Protasi,* Clara Franzini-Armstrong,* and Bernhard E. Flucher‡

*Department of Cell Developmental Biology, University of Pennsylvania, Philadelphia, Pennsylvania 19104-6058; and
‡Department of Biochemical Pharmacology, University of Innsbruck, A-6020 Innsbruck, Austria

Abstract. Rapid release of calcium from the sarcoplasmic reticulum (SR) of skeletal muscle fibers during excitation–contraction (e–c) coupling is initiated by the interaction of surface membrane calcium channels (dihydropyridine receptors; DHPRs) with the calcium release channels of the SR (ryanodine receptors; RyRs, or feet). We studied the early differentiation of calcium release units, which mediate this interaction, in BC_3H1 cells. Immunofluorescence labelings of differentiating myocytes with antibodies against α_1 and α_2 subunits of DHPRs, RyRs, and triadin show that the skeletal isoforms of all four proteins are abundantly expressed upon differentiation, they appear concomitantly, and they are colocalized. The transverse tubular system is poorly organized, and thus clusters of e–c coupling proteins are predominantly located at the cell periphery. Freeze fracture analysis of the surface membrane reveals tetrads of large intramembrane particles, arranged in orderly arrays. These appear concomitantly with arrays of feet (RyRs) and with the appearance of DHPR/RyS clusters, confirming that the four components of the tetrads correspond to skeletal muscle DHPRs. The arrangement of tetrads and feet in developing junctions indicates that incorporation of DHPRs in junctional domains of the surface membrane proceeds gradually and is highly coordinated with the formation of RyR arrays. Within the arrays, tetrads are positioned at a spacing of twice the distance between the feet. The incorporation of individual DHPRs into tetrads occurs exclusively at positions corresponding to alternate feet, suggesting that the assembly of RyR arrays not only guides the assembly of tetrads but also determines their characteristic spacing in the junction.

EXCITATION contraction (e–c)[1] coupling in muscle cells comprises a series of events linking depolarization of the plasma membrane to the release of calcium from the sarcoplasmic reticulum (SR; Schneider, 1981; Rios et al., 1991). Specific structures, named calcium release units, perform this functional interaction between SR and plasma membrane (Franzini-Armstrong and Jorgensen, 1994; Flucher and Franzini-Armstrong, 1996). Calcium release units are formed by the close apposition of specialized junctional domains of the SR on one side and of the plasma membrane, including its invaginations, the transverse (T) tubules, on the other. The junctional domains contain two key proteins involved in e–c coupling: the ryanodine receptor (RyR) of the junctional SR (for reviews see Sorrentino and Volpe, 1993; Meissner, 1994; and Coronado et al., 1994) and the dihydropyridine receptor (DHPR) located in the junctional domains of plasma membrane and T tubules (Jorgensen et al., 1989; Flucher et al., 1990; Yuan et al., 1991). The RyR is the SR calcium release channel (Imagawa et al., 1987; Inui et al., 1987; Lai et al., 1988). This molecule is composed of two different domains: the channel domain, inserted into the SR membrane, and the cytoplasmic domain, called the "foot." Feet form extensive ordered arrays (Franzini-Armstrong, 1970) and span the narrow gap between the membranes of SR and plasma membrane–T tubules (Block et al., 1988; Radermacher et al., 1994).

The DHPR is an L-type calcium channel that is responsible for initiating e–c coupling events by acting as a voltage sensor (Rios and Brum, 1987; Tanabe et al., 1988; Adams et al., 1990). According to the mechanical coupling hypothesis, interaction between the voltage sensor and the SR calcium release channel in skeletal muscle involves a direct functional link between the two proteins (DHPRs and RyRs; Schneider and Chandler, 1973). Strong support for this hypothesis comes from the observation that junc-

Please address all correspondence to Dr. Feliciano Protasi, Department of Cell and Developmental Biology, School of Medicine, University of Pennsylvania, Philadelphia, PA 19104-6058. Tel.: (215) 898-3345; Fax: (215) 573-2170; E-mail: protasi@mail.med.upenn.edu

1. *Abbreviations used in this paper*: DHPR, dihydropyridine receptor; e–c, excitation contraction; RyR, ryanodine receptor; SR, sarcoplasmic reticulum; T, transverse.

tional plasma membrane and T tubules are occupied by tetrads, groups of four integral membrane proteins, that are located exactly in correspondence to the four feet subunits (Block et al., 1988). If tetrads correspond to groups of four DHPRs, their alignment with the feet constitutes the basis for an interaction between DHPRs and RyRs. The lack of tetrads in dysgenic myotubes carrying a mutation of the DHPR (Franzini-Armstrong et al., 1991) and their reappearance after transfection with cDNA encoding for the DHPR (Takekura et al., 1994*a*) provided initial evidence for the identification of tetrads with DHPRs. One puzzling observation, however, is that tetrads are associated only with alternate feet, thus creating two categories of feet: those that are linked to tetrads and those that are not (Block et al., 1988; Franzini-Armstrong and Kish, 1995).

Recently a third component of the junction, called triadin, has received considerable attention (Caswell et al., 1991; Knudson et al., 1993*a*,*b*). This 95-kD SR protein is involved either in the interaction between RyRs and DHPRs (Brandt et al., 1990; Kim et al., 1990; Fan et al., 1995*a*,*b*) or in the association between RyRs and calsequestrin (Knudson et al., 1993*a*,*b*; Guo and Campbell, 1995). The latter is the calcium binding protein located in the lumen of the terminal SR cisternae (Meissner, 1975; MacLennan et al., 1983; Ikemoto et al., 1989; Pozzan et al., 1994).

BC_3H1 is a nonfusing cell line derived from a mouse brain tumor (Schubert et al., 1974). Withdrawal of growth factors induces these cells to differentiate by expressing several skeletal muscle-specific proteins (Taubman et al., 1989), including RyRs (Marks et al., 1989; Airey et al., 1991), and functional L-type calcium channels identified as DHPRs (Caffrey et al., 1987; Caffrey and Farach, 1988; Morton et al., 1988; Rampe et al., 1988). These cells were chosen for the study of calcium release unit development because they form extensive peripheral couplings, junctions between the SR and the plasma membrane (Marks et al., 1989, 1991). We sought to confirm that tetrads are composed of DHPRs and explored how tetrads and feet are assembled into coextensive arrays.

The present results show a striking correlation in the expression of DHPRs, RyRs, and triadin in the coclustering of these three junctional proteins and in the specific association of feet (RyRs) and tetrads (DHPRs) during development. The extensive junctional domains of BC_3H1 cells allow, for the first time, the use of optical diffraction to determine the spacing and orientation of tetrads, confirming that the disposition of tetrads is closely related to that of alternate feet. Interestingly, incomplete arrays of tetrads that are in the process of formation also show the alternate positioning of tetrads relative to feet, thus indicating that intrinsic molecular properties determine this arrangement.

Materials and Methods

Cell Culturing and Fixation

The BC_3H1 cell line was bought from American Type Culture Collection (Rockville, MD). The cells were grown in a growth medium containing low glucose DME medium (GIBCO BRL, Gaithersburg, MD), 20% fetal bovine serum, 0.5% chicken embryo extract, 100 U/ml penicillin, 100 mm/ml streptomycin, and additional 2 mM L-glutamine. Cells were plated on aclar (Pro-Plastics, Linden, NY), thermanox (Nunc Inc., Naperville, IL), or glass coverslips. Some coverslips were covered with matrigel (Collaborative Biomedical Products, Bedford, MA). BC_3H1 cells grow slightly faster on matrigel and they are better attached to the coverslip. This helps during fixation in which cells cultured directly on the coverslip tend to detach. The medium was changed every 2–3 d. At ~70% confluence, the growth medium was replaced by a low serum medium containing 0.5% fetal bovine serum and no chicken embryo extract (differentiation medium) to induce differentiation, and the cells were fixed 3–8 d later.

Immunohistochemistry

Cultures grown on glass coverslips were fixed and immunostained as previously described (Flucher et al., 1993*b*). Methanol-fixed cultures were incubated with 10% normal goat serum in PBS containing 0.2% BSA (PBS/BSA) for 30 min and then incubated in primary antibodies for at least 2 h at room temperature or overnight at 4°C. After washing in five changes of PBS/BSA the cultures were incubated in fluorochrome-conjugated secondary antibodies (Cappel Laboratories, Malvern, PA) for 1 h at room temperature and washed again. Controls were performed in which the primary antibodies were omitted or were composed of an inappropriate antibody combination (mouse primary with anti–rabbit secondary and vice versa). The glass coverslips were then mounted in 90% glycerol, 0.1 M Tris, pH 8.0, with 5 mg/ml *p*-phenylenediamine to retard photobleaching. The specimens were viewed and photographed with black and white film on a light microscope (Axioskop or Axiovert; Carl Zeiss, Thornwood, NY) equipped with epifluorescence optics. Pictures were digitized by scanning the negative film, and the contrast and density of the pictures were optimized with image processing software (Adobe Photoshop, Adobe Systems Inc., Mountain View, CA). The working dilutions and the sources of primary antibodies are listed in Table I. All antibodies have been fully characterized and used on cultured skeletal myotubes in the quoted literature.

Electron Microscopy

Cells grown on either type of plastic coverslip were washed twice in PBS at 37°C, fixed in glutaraldehyde, and kept in fixative for up to 1–4 wk before further use. For thin sectioning, two different protocols were used: (*a*) 3.5% glutaraldehyde in 0.1 M sodium cacodylate buffer, pH 7.2, followed by 2% OsO_4 for 2 h at room temperature and saturated uranyl acetate for 4 h at 60°C; (*b*) 2.5% glutaraldehyde and 1% tannic acid for 1 h followed by extensive washes in buffer; 1% OsO_4 for 2 h at 4°C; and 0.5% uranyl acetate for 2 h at room temperature. The samples were embedded in Epon 812 and the sections stained either in saturated aqueous uranyl acetate or in 1% uranyl acetate followed by lead salts, both for 8 min.

For freeze fractures, the cells were fixed in glutaraldehyde as in (*a*) above and infiltrated in 30% glycerol. A small piece of the coverslip was mounted with the cells facing a droplet of 30% glycerol, 20% polyvinyl alcohol on a gold holder and frozen in liquid nitrogen-cooled propane (Osame et al., 1981). The coverslip was flipped off to produce a fracture that followed the culture surface originally facing the coverslip. The fractured surfaces were shadowed with platinum either at 45° unidirectionally or at 25°C while rotating and replicated with carbon in a model BFA 400 Balzers freeze fracture. Sections and replicas were photographed in an electron microscope (410; Philips Technologies, Cheshire, CT).

Results

Immunohistochemistry

Cultured BC_3H1 cells were immunolabeled with antibod-

Table I. Antibodies Used and Their Specificity

Specificity (code)	Type	Dilution	Reference
RyR (#5)	Rabbit, affinity purified	1:5,000	Flucher et al., 1993*b*
α_1 DHPR (1A)	Mouse monoclonal	0.1 μM	Morton and Froehner, 1987
α_2 DHPR (20A)	Mouse monoclonal	0.1 μM	Morton and Froehner, 1989
Triadin (GE 4.90)	Mouse monoclonal	15 μg/ml	Caswell et al., 1991
T tubules (TT2)	Rabbit, affinity purified	1:800	Flucher et al., 1991

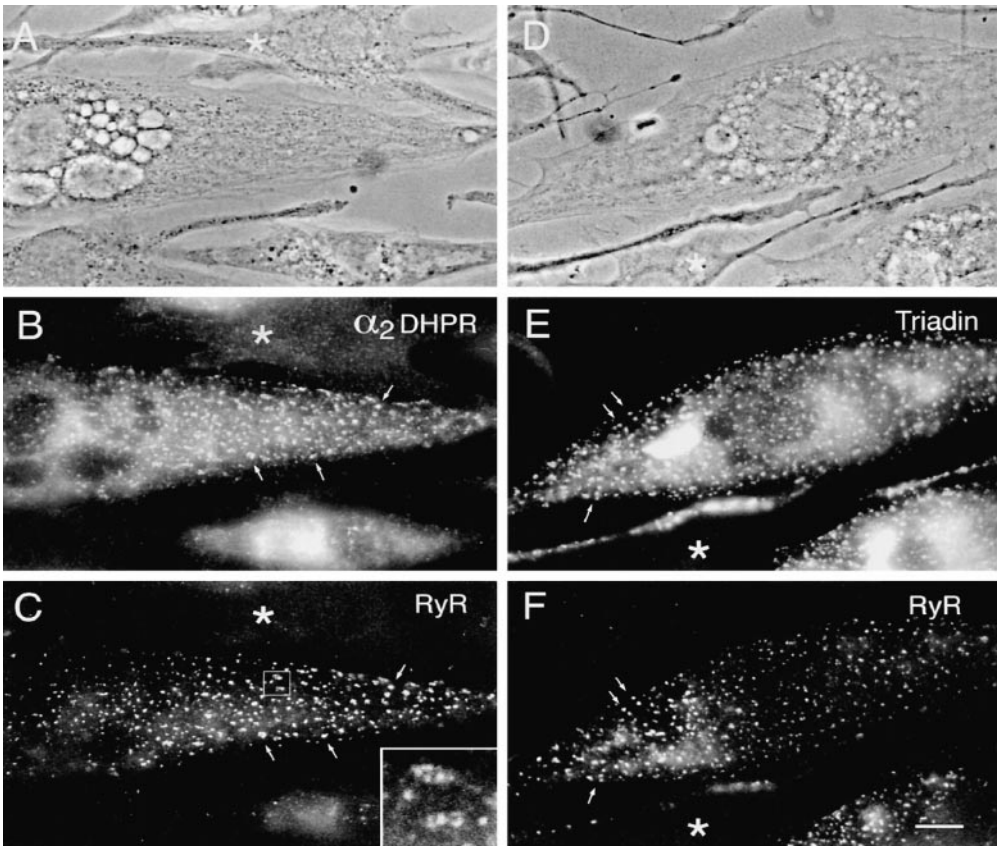

Figure 1. Double-immunofluorescence labeling of triad proteins in differentiated BC_3H1 cells. 4 d after change to low serum medium (D4) many cells have assumed a spindle shape and express triad proteins, whereas other cells remain undifferentiated (*asterisks*). Both the DHPR α_2 subunit (*B*) and triadin (*E*) are colocalized with the RyR (*C* and *F*) in clusters at or close to the cell surface, indicative of plasma membrane–SR junctions. The shapes and the distribution of the immunolabeled clusters correspond highly with one another in the double-labeled pairs (examples indicated by *arrows* in *B*, *C*, *E*, and *F*). Some clusters are unusually large and are composed of multiple subdomains (see *inset* in *C* at 4-fold higher magnification). (*A* and *D*) Phase contrast images of fields shown in *B*, *C*, *E*, and *F*, respectively. Bar, 10 μm.

ies specific for two proteins of the junctional SR: the RyR and triadin (95-kD protein); for proteins of the junctional T tubules or plasma membrane: the DHPR (α_1 and α_2 subunits); and for a general T tubule antigen of unknown identity (Flucher et al., 1991). Before change to low serum medium, BC_3H1 cells were negative for all antibodies used (not shown). 4 d after serum withdrawal (D4), numerous spindle-shaped differentiated cells reacted with the antibodies against the junctional proteins (Figs. 1 and 2). About 40% of the cells differentiate, as indicated by the expression of junctional proteins (115 out of 283 cells in 15 randomly chosen fields from two coverslips; ~0.5 mm^2 area). The α_1 and α_2 subunits of the DHPR, the RyR, and triadin are located in numerous discrete clusters at the periphery of the cell, whereas focusing up and down through the cells showed that little to no specific immunolabel was found in the cytoplasm. Double immunolabeling of RyRs with either α_1 and α_2 subunits of DHPRs or triadin shows the colocalization of all four proteins within surface clusters (Figs. 1 and 2). The immunofluorescent clusters are variable in size, some of the aggregates being quite large compared to those seen in normal myotubes in vitro (Flucher et al., 1994) and occasionally appear to be composed of several subdomains (Fig. 1 *C*, *inset*). In double labeling experiments, the sizes and shapes of corresponding RyR/DHPR or RyR/triadin clusters agree well with one another, indicative of a parallel incorporation of triad proteins into SR–surface membrane junctions.

Immunostaining for a general T tubule protein gave negative results (Fig. 2 *D*) even in cells that are differentiated, as indicated by the presence of DHPR-positive clusters. The great majority of the junctional protein clusters appear on or near the surface membrane, both on the ventral, substrate-facing and the dorsal sides of the cells.

Electron Microscopy

Thin Sections: Arrays of Feet. Consistent with the immunolocalization, BC_3H1 cells have few internal junctions but numerous peripheral couplings (SR–surface junctions) of variable size, many larger than those seen during differentiation of normal myotubes (Fig. 3, compare with Pincon-Raymond et al., 1985; Flucher et al., 1993*b*, 1994; Takekura et al., 1994*b*). Some junctional gaps have none or few identifiable feet, many have small arrays of regularly spaced feet occupying only part of the gap (Fig. 3 *A*, *arrows*), and others are entirely filled with arrays of feet (Fig. 3, *B* and *C*, *arrows*). The average distance between feet measured in thin section images showing very distinct profiles is 31.0 ± 3.5 nm (mean ± 1 SD; number of junctions = 47).

Freeze Fracture: Clustered Tetrads. The fracture plane follows the cell membrane facing the substrate (the same as shown and analyzed in the immunofluorescence experiments; Figs. 1 and 2). In undifferentiated cultures, the cells are odd shaped and smaller; after withdrawal of growth factors, larger, spindle-shaped cells similar to those positive for antibodies against junctional proteins (Figs. 1 and 2) become numerous, but undifferentiated cells are still present.

The cytoplasmic leaflet in undifferentiated cells is characterized by randomly disposed intramembrane particles

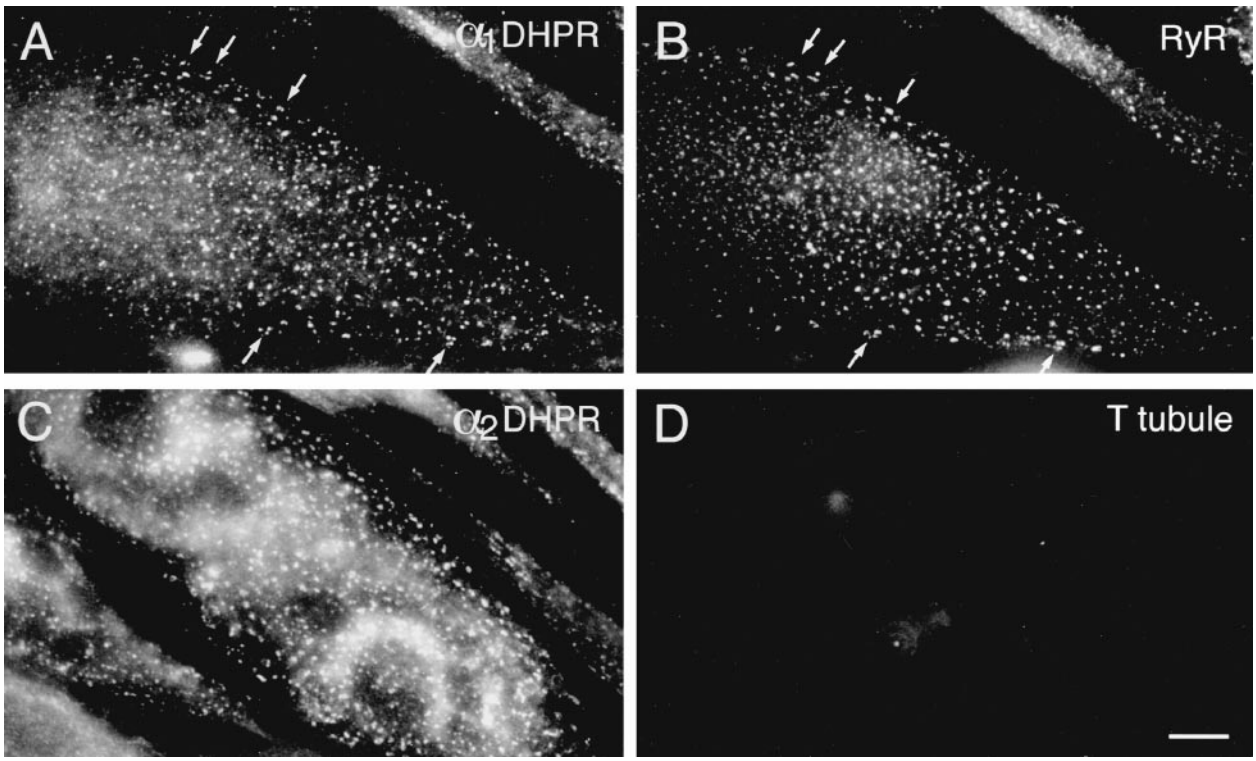

Figure 2. Double-immunofluorescence labeling of DHPR α_1 and α_2 subunits with the RyR and a general T tubule marker. In differentiated BC_3H1 cells (D4), clusters of α_1 DHPRs (*A*) and RyRs (*B*) are colocalized at or close to the cell surface (examples indicated by *arrows*). The colabeled clusters most likely represent peripheral couplings between the SR and either the plasma membrane or short invaginations. Cells that express clusters of α_2 DHPR (*C*) do not express the nonjunctional T tubule proteins labeled with the antibody TT2 (*D*), indicating that a mature T system is not present in differentiated BC_3H1 cells. Bar, 10 μm.

and lack of caveolae or other membrane invaginations (Fig. 4 *A*). Only 1 out of 138 observed cells in the growth phase, or 0.7% (from three coverslips, two cultures), had few shallow plasma membrane mounds where large particles were clustered at a somewhat higher density (Fig. 4 *B*). The clusters in this single cell had a low density, and they contained few large particles; and it is questionable whether occasional groups of large particles are equivalent to tetrads (Fig. 4 *B*, *circle*). Upon differentiation, numerous cells show two characteristic changes: the presence of frequent clusters of tall particles with large diameters and openings of membrane invaginations (compare Fig. 4, *A*, undifferentiated, with *C*, differentiated). About 40% of the cells (41.3% of the 804 cells from 19 replicas of 9 cultures) have clusters of large particles in cultures exposed to differentiation medium for 3–8 d. This is in agreement with immunofluorescence.

The particle clusters in differentiated cells contain regular arrays of tetrads (Figs. 5 and 6). Three criteria define tetrads: (*a*) a complete tetrad is composed of four large membrane particles positioned at the corners of squares with a distance of 17 to 18 nm between the centers of adjacent particles (Fig. 5, lines *A* and *B*); (*b*) tetrads always occur in groups forming orthogonal arrays with a distance of ~41 nm between the centers of adjacent tetrads (Fig. 6, *C* and *E*, and see below); and (*c*) particles outside their designated positions at the corners of the squares are usually excluded from the membrane within tetrad arrays (Fig. 6). These characteristics allow the unequivocal recognition of tetrads even if one criterion is not fully met. For instance,

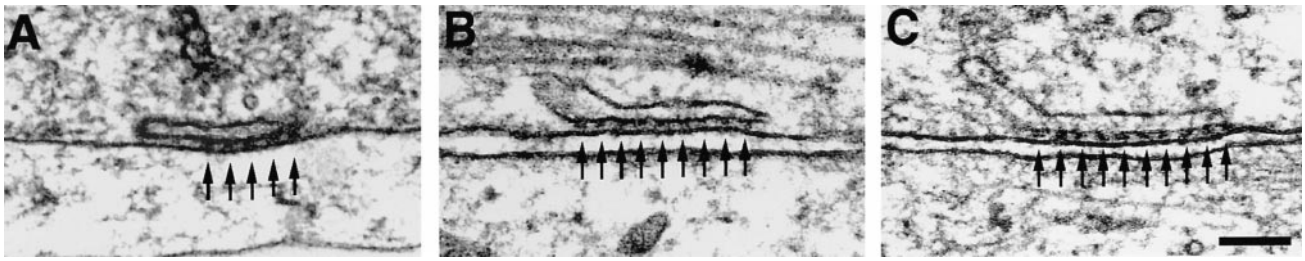

Figure 3. Thin sections showing the periphery of differentiated BC_3H1 cells (D3–D8). Peripheral couplings are formed by an SR cisterna associated with the plasma membrane. Arrays of feet, positioned at regular intervals (*arrows*), occupy only part of the junction in *A* but the whole junction in *B* and *C*. Bar, 0.1 μm.

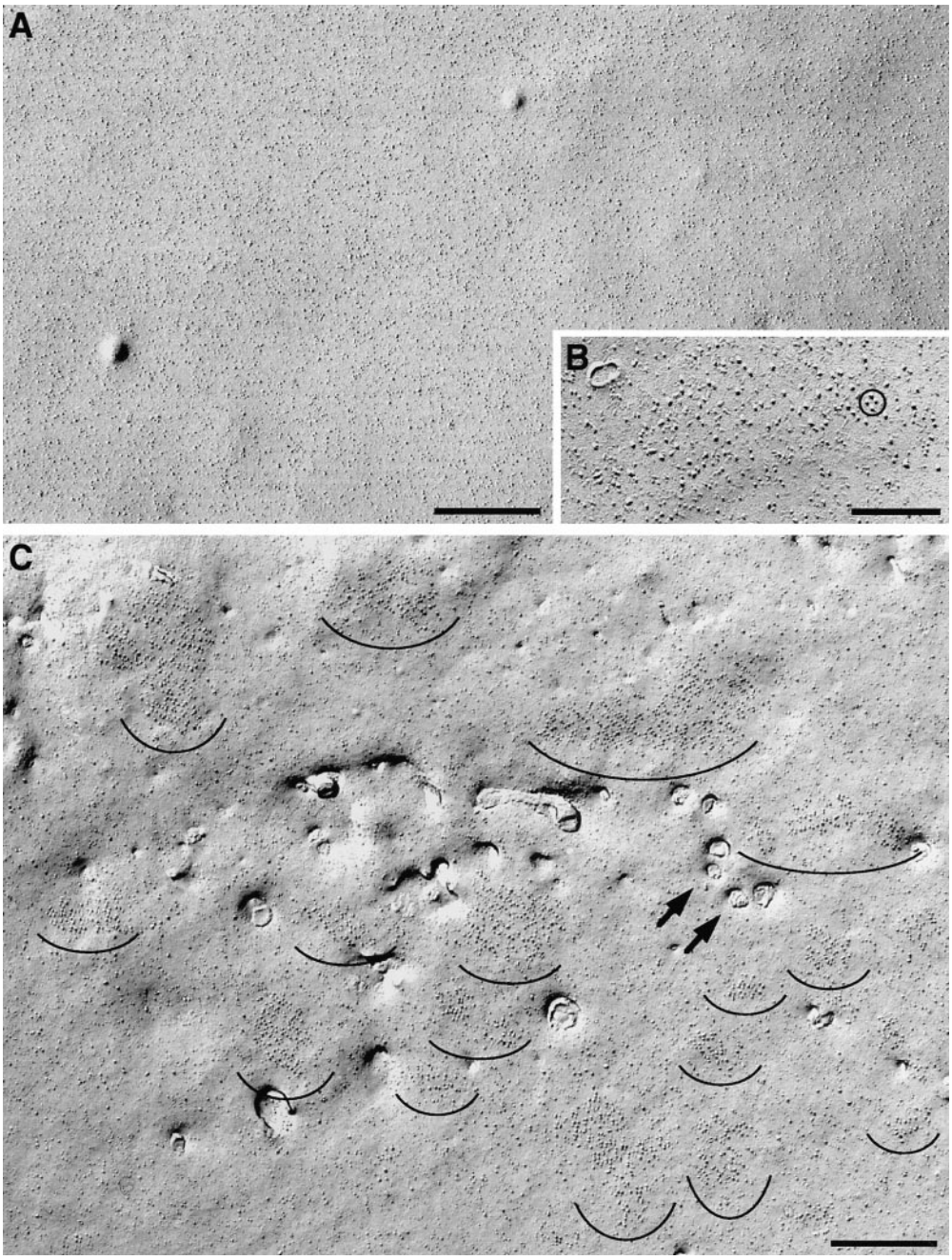

Figure 4. Freeze fracture replicas of the plasmalemma from cells in growth medium (*A* and *B*) and from a differentiated cell (D6; *C*). Undifferentiated cells have a smooth surface with uniform distribution of intramembrane particles (*A*), while ~41% of cells in differentiation medium have numerous clusters of large intramembrane particles (*C*, *semicircles*). Within the clusters, the particles form groups of four (tetrads). Only 1 of the 138 cells examined in growth medium contained small clusters of large particles, occasionally grouped as in a tetrad (*B*, *circle*); these may be precursors of the larger, more crowded clusters of differentiating cells. Openings of surface invaginations (*arrows*) are present only in differentiated cells. Smaller openings probably belong to primitive T tubules and larger ones to shallow membrane invaginations. Invaginations are infrequent, particularly in early (D3–D5) cells. Bars: (*A* and *C*) 0.5 μm; (*B*) 0.2 μm.

the "square" can become slightly distorted during fracturing (Fig. 5 *E*, *1* and *2*), or some of the particles may be missing from the corners (Fig. 5, *C–E*). Complete or incomplete (three large particles) tetrads are practically never found in cells in growth medium (see above) and are not found in cells that, although grown in differentiation medium, appear undifferentiated, as indicated by the absence of membrane invaginations and overall scarcity of membrane particles. Arrays of tetrads mostly occur on plasma membrane mounds that presumably represent the areas of close SR apposition.

The distortions of tetrads and the lack of one or more particles may either arise from common freeze fracture artifacts or reflect an incomplete or imperfect molecular assembly. To interpret our data in terms of junction assembly we need to distinguish between these two possibilities. The distortion and slight misplacement of particles (Fig. 5 *E*, *1* and *2*) are similar to artifacts often seen in freeze fracture images, and we assume that they do not reflect any structural defect of the proteins. Missing particles are often substituted by short stumps (Fig. 5, *C* and *D*), which may represent proteins broken during fracturing. In areas where the arrays appear most complete, small stumps are almost invariably present, indicating that these arrays were more complete than they may seem on a superficial examination. Some missing particles are not substituted by stumps (Fig. 5 *E*, *3* and *4*), and thus the protein was probably absent from that position. In areas where the arrays appear most incomplete, missing particles are less frequently substituted by stumps (Fig. 5 *E*, *3* and *4*). In these areas the

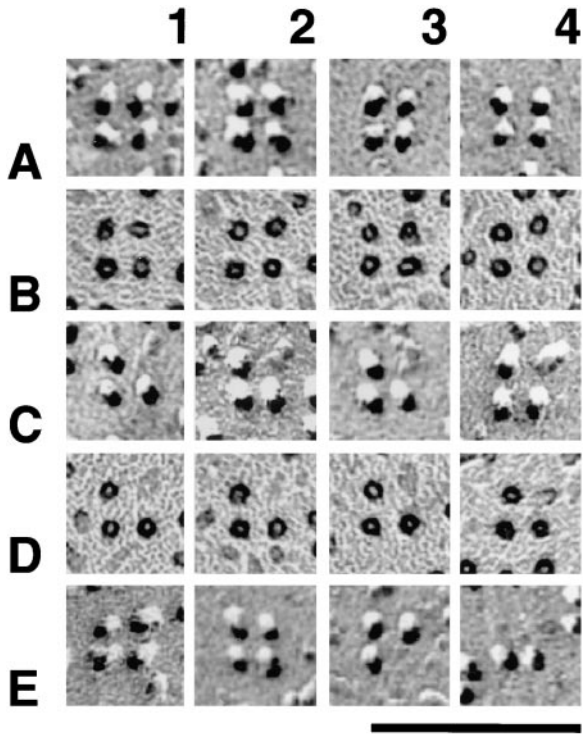

Figure 5. Montage of tetrads either unidirectionally (*A*, *C*, and *E*) or rotary (*B* and *D*) shadowed. A tetrad is composed of four equal intramembrane particles disposed at the corners of a square with a center-to-center spacing of 17 to 18 nm between particles. The particles have a large diameter, and the elongated platinum-free "shadow" indicates that they are tall. Incomplete tetrads apparently miss one or more particles, but short, distorted stumps in place of the missing particles indicate that the protein was present before fracturing (*C* and *D*). Some tetrads truly miss a component, since no stump is visible in the place of a missing particle (*E*, *3* and *4*). The whole tetrad may become distorted during fracturing, resulting in an asymmetric shape (*E*, *1* and *2*). Bar, 0.1 μm.

tetrads may be in the process of assembling and thus may lack many components, or, less likely, be in the process of disassembling (see Discussion).

Analysis of Tetrad Arrays. Large clusters of tetrads are often made up of several subdomains with distinct orientations of their arrays. This could result from multiple and independent initiation sites for the formation of arrays within one cluster. We first analyzed the parameters of well differentiated tetrad arrays. Centers of tetrads could easily be identified and marked with a dot in areas with fairly complete clusters, even though some tetrads were partially distorted and missed some components (Fig. 6, *C* and *E*). This generated orthogonal arrays of dots with a spacing of 41.2 ± 3.1 nm (mean ± 1 SD) along the orthogonal axes (Fig. 6 *E*, *dashed lines*) and 58.4 ± 4.7 nm along the diagonals (Fig. 6 *E*, *arrows*). The latter spacing is approximately twice the spacing between the feet measured in thin sections.

The ordered disposition of tetrads in arrays was confirmed by optical diffraction analysis. In images of rotary-shadowed replicas (Fig. 7 *A*), the position of each particle is precisely marked by the symmetric ring of platinum shadow around it, thus making the array an appropriate object for optical diffraction. The pattern of reflections in the diffraction pattern (Fig. 7 *B*) was indexed by two orthogonal lattices with spacings of 1/18.4 ± 0.4 and 1/41.9 ± 1.6 nm (mean ± 1 SD, the average of 5 to 6 patterns from different particle clusters). The two values correspond, respectively, to the distance between particles in the tetrad and to the center-to-center distance between tetrads, as measured in the micrographs. The angle between the two lattices, 65.5 ± 0.5°, corresponds to the skew angle between lines joining the centers of tetrads and those joining the centers of particles within a tetrad (Franzini-Armstrong and Kish, 1995). The significance of the two lattices was determined by comparison with diffraction patterns derived from a model of tetrad arrays (Fig. 7 *C*). The model is built by exactly superimposing tetrads over alternate feet in an array constructed as in Takekura et al. (1994*a*) and Franzini-Armstrong and Kish (1995). The main feature of the model is the skew angle between the orthogonal array formed by tetrad centers and that of the four tetrad subunits, which is determined by the underlying disposition of feet. The diffraction pattern of this model (Fig. 7 *D*) indexes on two orthogonal lattices with spacings inversely proportional to the center-to-center distances between the adjacent tetrads and between the particles composing the tetrads. The two lattices in the diffraction pattern are skewed by an angle of 71.5°. Thus the array of tetrads in the freeze fracture images is composed of groups of square (or quadrate) units disposed in an orthogonal array with a skewed disposition, just as in the model.

The analysis of subdomains with many incomplete tetrads provides further information about the relationship between the organization of individual tetrads and their arrays. Using a procedure similar to the one described above allowed us to designate particles belonging to a tetrad by their position adjacent to dots of an orthogonal array with a spacing of 41 nm (Fig. 8, legend). Two examples of small arrays with few particles are shown in Fig. 8, *A* and *B*. The great majority (96%) of large membrane particles in the clusters was located in correct positions of putative tetrads regardless of how complete the tetrads were (Fig. 8). The incidence of free particles apparently not part of a tetrad was low and independent of the particle density (or occupancy), which ranged from 15 to 89% of the maximal possible number of tetrad particles in 88 analyzed subdomains. We conclude that particles in the subdomains are predominantly positioned at the sites of tetrads, that is, in correspondence to alternate feet, even when the arrays of tetrads are quite incomplete. The same analysis applied to randomly disposed particles in peripheral clusters of cardiac myocytes, which do not form tetrads at all (Sun et al., 1995; Protasi et al., 1996), gives a high number of particles that could not be associated with putative tetrad centers. In addition, the frequency of these random particles is strongly dependent on the overall density of particles (Fig. 8), indicative of an accidental positioning near tetrad centers. Thus, the analysis procedure used can distinguish between randomly disposed particles and incomplete arrays of tetrads and therefore provides a quantitative measure for the degree of tetrad assembly.

Correspondence between Arrays of Tetrads and Feet. Numerous similarities between arrays of feet seen in thin sec-

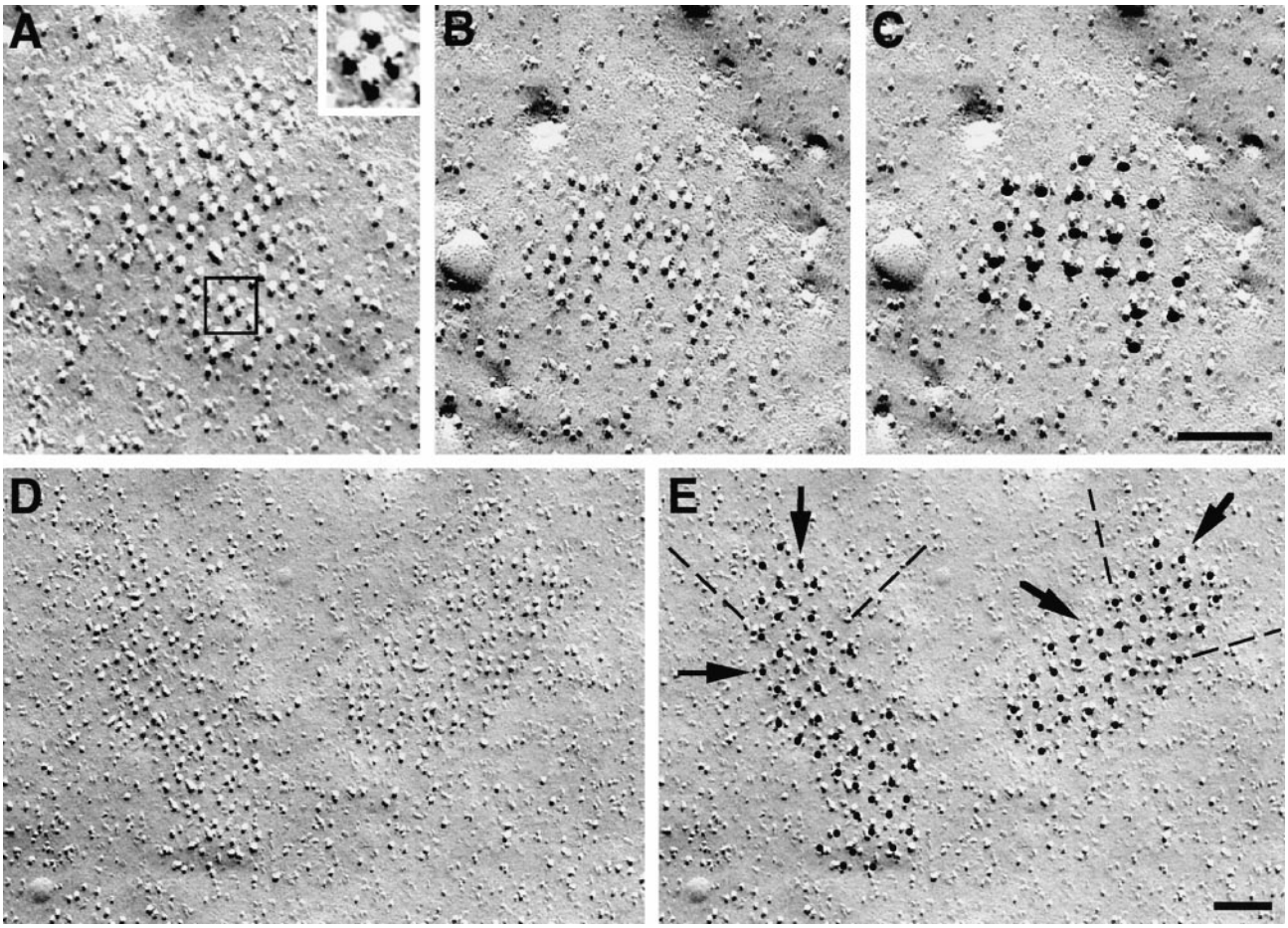

Figure 6. Tetrads, whether perfectly preserved or distorted during fracturing, are identified on the basis of their position in arrays. Once a tetrad is identified in *A* (*square*, and at higher magnification in *inset*) it is easy to see that equally oriented adjacent tetrads are located in an orthogonal arrangement around it. Marking the tetrads by putting a dot in their centers helps in identifying the pattern. In *B–E* the tetrads (including those that miss one or two components) are marked in the second of the two identical images (*C* and *E*). The dots define an orthogonal arrangement with a center-to-center spacing between adjacent tetrads of ~41 nm (*E*, along the *dashed line*). The spacing along the diagonals (*E*, *arrows*) is ~58 nm. Bars, 0.1 μm.

tions and the arrays of tetrads detected by freeze fracture suggest that both molecular assemblies belong to a single underlying cytoplasmic structure and that they develop concomitantly. (*a*) Both arrays are rarely seen in undifferentiated cells but frequently observed in differentiated cells. (*b*) Both structures occur in variable sizes. (*c*) Particle clusters occupy a patch of membrane that is slightly raised into a shallow, flat mound indicative of the apposition of an SR cisterna underneath. (*d*) In some junctions, feet and tetrad particles occupy only a portion of the junction (Fig. 9, *A* and *B*). (*e*) Multiple subdomains of feet in individual peripheral couplings and multiple subdomains of tetrads in the large particle clusters indicate that both proteins become organized in the junctions starting from multiple seed points. This is illustrated in Fig. 9, *C* and *D*, showing a large cluster of particles composed of several minidomains with different orientations of tetrad arrays (Fig. 9 *C*, *arrows*) and a junctional gap containing two separate groups of feet with different orientations (Fig. 9 *D*, *arrows*). (*f*) The diffraction pattern from arrays of tetrads and the spacing between tetrads are entirely compatible with a model of tetrad disposition based on a 1:2 ratio of tetrads to feet. The measured spacing between tetrads along the diagonal of the orthogonal array is twice the measured spacing between feet, as predicted by this model.

Correspondence of Clusters of Feet and Tetrads with Clusters of Immunolabeled RyRs and DHPRs

Immunoreactive clusters of RyRs and DHPRs share several characteristics with clusters of feet and tetrads as seen in electron microscopy. First, all are absent in cells during the proliferating phase, but they appear simultaneously in an increasing portion of BC_3H1 cells upon differentiation. Secondly, DHPR/RyR immunoclusters are located almost exclusively at the periphery of the cells and occur at similar densities as clusters of tetrads. For example, the cells shown in Figs. 1 *C* and 2 *B*, which are good examples of well differentiated cells with numerous clusters, have cluster densities of 314 and 213/1,000 μm^2, respectively. These clusters mainly represent peripheral couplings, since EM of cells at comparable stages of differentiation shows very few primitive T tubules forming junctions that are located immediately below the cell surface. The density of immu-

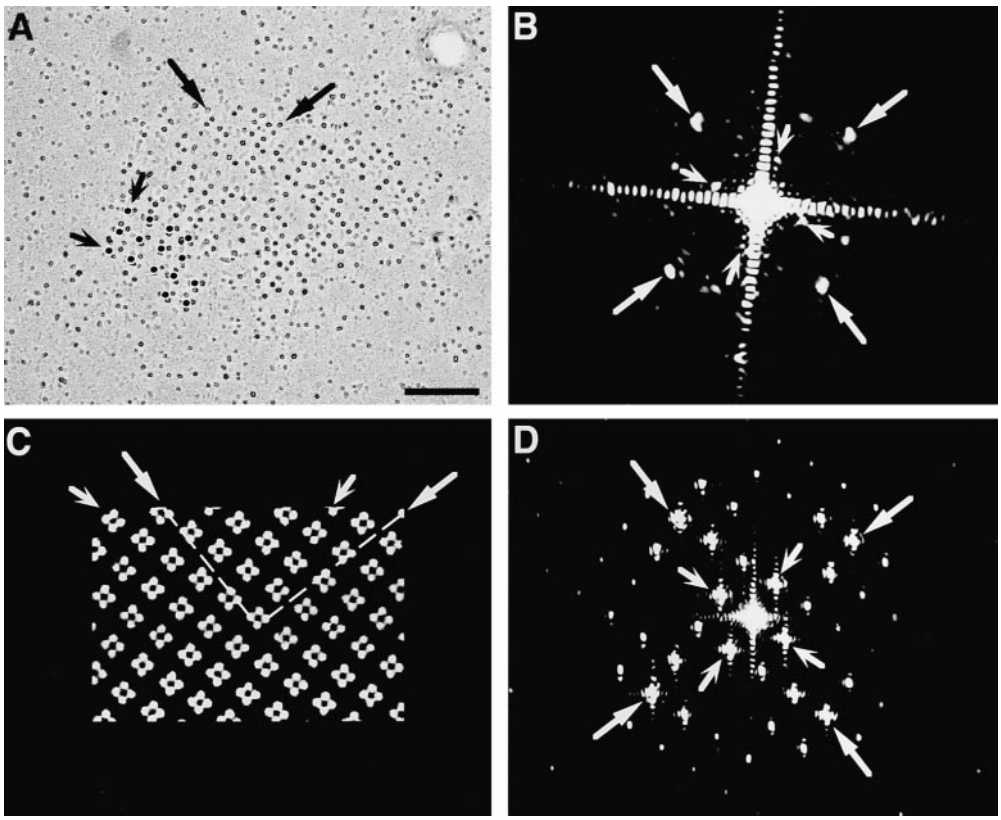

Figure 7. Images and optical diffraction patterns of a rotary-shadowed tetrad cluster (*A* and *B*) and of a model array, constructed by exactly positioning tetrads over an array of feet, in correspondence of every other foot (Franzini-Armstrong and Kish, 1995; *C* and *D*). The position of each tetrad particle is marked by a small ring of platinum shadow in *A* and modeled by a filled circle in *C*. Alignment of the particles is visible by holding the micrograph at eye level and glancing along the axes indicated by the arrows. Small, winged arrows in *A* and *C* indicate alignment of tetrad centers along the sides of an orthogonal array with a spacing of ~41 nm. See also Fig. 6. The diffraction pattern of the freeze fracture (*B*) indexes on two orthogonal lattices skewed relative to each other, with spacings of ~1/42 (*small*, *winged arrows*) and ~1/18 nm (*large arrows*), corresponding to the distance between the centers of adjacent tetrads and of the particles within the tetrads, respectively. The diffraction pattern from the model also indicates two orthogonal lattices with spacings corresponding to those between the centers of tetrads (*small*, *winged arrows*) and the centers of tetrad subunits (*large arrows*). The angle between the two lattices in the diffraction pattern from the tetrad arrays (65–66°) differs only slightly from that of the model array (71.5°). Bar, 0.1 μm.

noclusters is in good correspondence with densities of tetrad clusters ranging between 183 and 278/1,000 μm^2 measured in freeze fracture replicas of well differentiated cells from cultures of the same age. Thirdly, with both techniques the clusters in BC_3H1 cells are found to be variable in size and often considerably larger than the corresponding clusters in normal myotubes developing in vivo and in vitro (compare with Pincon-Raymond et al., 1985; Flucher et al., 1993*b*, 1994; Takekura et al., 1994*b*). And finally, large DHPR/RyR clusters are sometimes composed of several smaller subdomains that may correspond to tetrad clusters with widely spaced subdomains.

Discussion

Assembly of the e–c coupling apparatus is an early event during skeletal muscle differentiation (Flucher, 1992). Studies with BC_3H1 cells have shown that transcription of mRNAs for RyR1 and the skeletal form of DHPR is initiated briefly after withdrawal of growth factors (Rampe et al., 1988; Marks et al., 1989). The present study adds triadin to the list of junctional proteins that are concomitantly expressed in the early differentiation process. Furthermore, all three proteins (RyR, DHPR, and triadin) assemble into junctional complexes essentially as soon as they are synthesized. Parallel appearance during development of DHPR clusters detected by immunocytochemistry and of arrays of tetrads as seen by freeze fracture analysis, as well as similar densities of both structures in differentiated myocytes, gives strong support to the identification of the tetrads as groups of four DHPRs.

Development of calcium release units in the nonfusing cell line BC_3H1 cells is independent of myoblast fusion, and in this sense it resembles myofibrillogenesis, which has also been shown to be independent of the fusion process. However, BC_3H1 lack α actinin, a major component of the Z lines, and I-Z-I brushes, that is, the association of thin filaments with Z lines (Holtzer et al., 1997). The observation that in BC_3H1 cells some aspects of e–c coupling development and myofibrillogenesis, such as the formation of peripheral couplings and A bands, occur normally whereas other aspects, like T tubule and Z line formation, are deficient may be indicative of at least two parallel regulatory mechanisms during early myogenesis, one of which is lacking in these cells. However, the deficiencies in the development of the muscle-specific cytoskeleton and membrane system may also be causally related, since the e–c coupling membranes become anchored at the Z lines during early sarcomere formation (Flucher et al., 1992, 1993*a*). Thus lacking Z lines could uncouple the internalization of the e–c coupling apparatus leading to the exceptional development of peripheral couplings and paucity of dyads and triads in BC_3H1 cells.

Most of the peripheral couplings in BC_3H1 cells do not have full assemblies of feet and tetrads. The number of cells with junctions, the density of junctions per cell, and

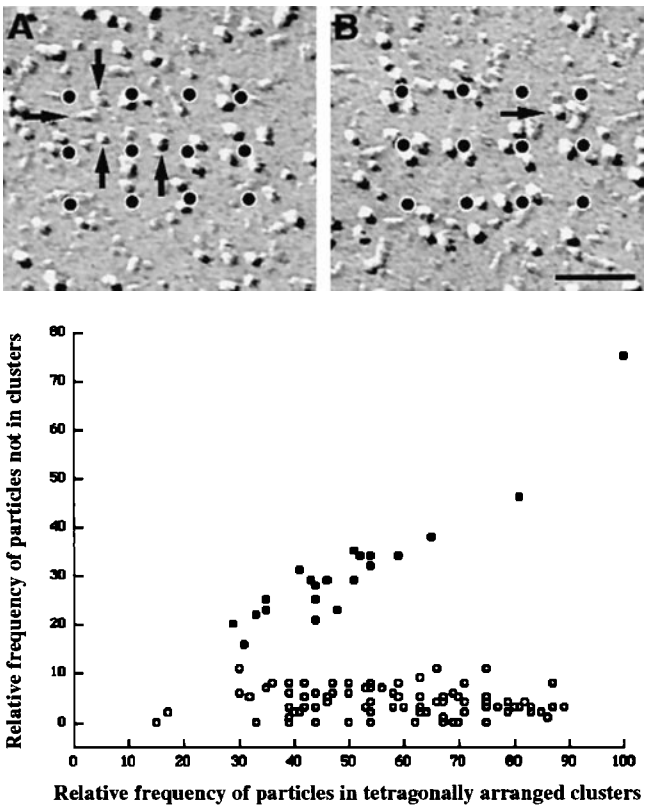

Figure 8. Arrangement of particles in tetrad arrays is not dependent on degree of completeness of tetrads. (*Graph*) Comparison of particle clustering in cardiac junctions (*filled circles*, randomly distributed particles) and BC_3H1 junctions (*open circles*, particles forming tetrads); each circle represents data from one continuous cluster of particles. (*Abscissa*) Relative frequency of particles that were closely associated to an orthogonal array of dots at a spacing of 41 nm. (*Ordinate*) Relative frequency of particles not associated with the array. Values are expressed as percentage of the maximal possible number of particles constituting tetrads within the junction area (4 × the number of dots). In BC_3H1 cells, the percentage of nonassociated particles is constant, and on average only 4% of the particles cannot be assigned to a tetrad position, regardless of the degree of filling of a junction (15–89%). In the random clusters of cardiac muscle, the frequency of particles not positioned at tetrad locations is higher and increases with the overall density of particles. Analysis procedure: subdomains of large clusters of particles in micrographs from cells at D3–D7 were overlaid with the array of dots and rotated to achieve maximal proximity of particles and dots. Particles were scored as either clustered around the dots, corresponding to the expected position in a tetrad (*abscissa*), or as distant to dots without apparent relationship to a tetrad (*ordinate*). Fig. 8, *A* and *B* shows two examples of incomplete arrays, with "dotted" tetrads. In *A* there are 18 particles clustered near the dots, or 37% of the 48 particles needed for a complete tetrad array. Arrows indicate four misplaced particles (or 8%). The values for Fig. 8 *B* are 50 and 2%. Particles at the edge of the array are not counted. Dotted arrays in Fig. 6 *E* fell in the 80–90% complete category. Data for cardiac junctions were obtained from micrographs constituting that data base in Sun et al. (1995) and Protasi et al. (1996). Bar, 50 nm.

the completeness of assemblies of tetrads and feet within the junctions all increase in parallel between days 3 and 6–7 of differentiation. Thus, junctions with incomplete assemblies most likely are in the process of formation. Whereas incomplete assemblies could also be indicative of degenerative processes, we would expect degradation to increase and not decrease with age. If assembly and disassembly of junctions occur simultaneously, the rate of assembly must exceed that of disassembly to yield an overall increase in junctions. Furthermore both processes have to proceed through structurally identical stages, since only one pattern of incomplete junctions has been observed. Therefore, we believe that the analysis of incomplete assemblies of tetrads and feet is relevant for understanding the process of junction formation.

The developmental analysis of the junctional complexes between SR and surface membrane in BC_3H1 cells is consistent with the identification of feet as RyRs and tetrads as groups of four DHPRs. The parallel appearance during development of several structural and molecular components , such as feet, tetrads, and immunoclusters, indicates the coordinated assembly of RyRs and DHPRs in the adjacent membrane domains of the undifferentiated SR–surface membrane junctions. Arrays of feet in the junctional SR membrane and of tetrads in the surface membrane often form around multiple, independent initiation points within single large junctions, resulting in several subdomains with different orientations. This suggests a mechanism of assembly by gradual incorporation of the junctional proteins into a preformed narrow junctional gap followed by their arrangement into extended arrays. The assembly could occur simultaneously at several points of one junction, and the separate arrays would eventually converge into one large array containing several subdomains. Alternatively, this pattern could result from the assembly of junctions from several preassembled junctional segments (Yuan et al., 1991). However, this mechanism would also require the simultaneous fusion of the underlying SR compartment, which is not consistent with the observed SR–plasma membrane junctions without feet. Given the ability of RyRs to self assemble into ordered arrays (Takekura et al., 1995), their normal assembly into T tubule–SR junctions without DHPRs in dysgenic myotubes (Powell et al., 1996), and the dependence of DHPRs on RyRs for achieving a related ordered arrangement (Protasi, F., C. Franzini-Armstrong, and P.D. Allen, unpublished observations; for review see Flucher and Franzini-Armstrong, 1996), we would expect that the organization of the feet array precedes and probably drives the formation of tetrads.

Previous analysis of the disposition of tetrads relied on direct observation and identification of individual tetrads, which was often hampered by missing components. Optical diffraction, on the other hand, detects the underlying order even where individual components are missing. This analysis shows that tetrads, even if incomplete, are spaced at distances that correspond to those of alternate feet and that tetrad position is skewed relative to the orthogonal axes of the array, as expected from an exact superimposition of tetrad particles over feet subunits (Franzini-Armstrong and Kish, 1995).

The spacing between the centers of adjacent particles of

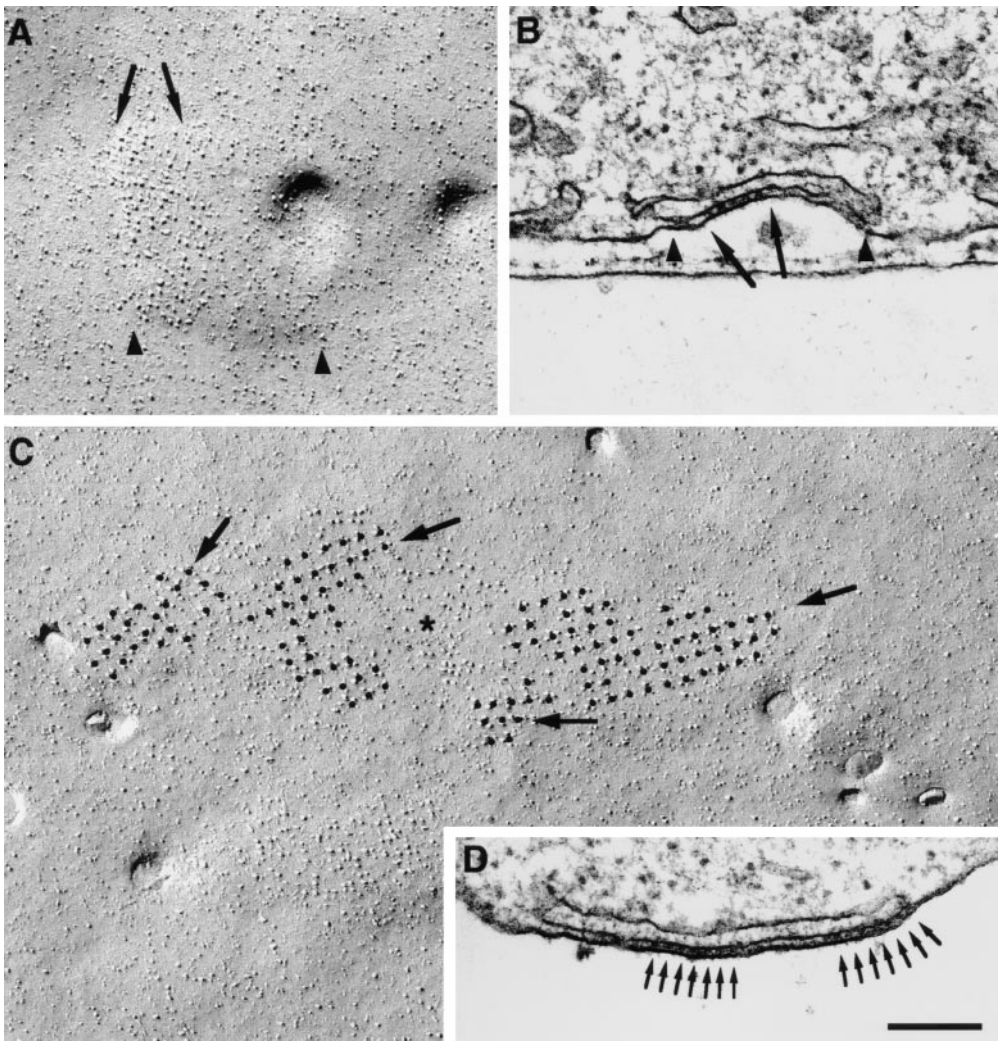

Figure 9. Comparison between arrays of particles and of feet. (*A*) An array of particles covers approximately half (between *arrows*) of a domed membrane domain (between *arrowheads*). (*B*) This corresponds to peripheral couplings (between *arrowheads*) in which only a portion of the junctional gap is occupied by an array of feet (between *arrows*). (*C*) A very large cluster of particles contains several subdomains of tetrads with different orientations (*arrows*), separated by spaces with fewer particles (*asterisk*). (*D*) A peripheral coupling containing two separate arrays of feet (*arrows*) with slightly different orientations. In fact, feet are better delineated at right than at left of the junction, indicating different orientations of the two arrays relative to the plane of the section. Bar, 0.2 μm.

a tetrad (~18 nm) is larger than the center-to-center distance between foot subunits (~14.5 nm; Radermacher et al., 1994), indicating that the centers of the DHPR particles are closer to the corners of a foot than to their centers. One consequence of this is that complete tetrads may not be able to fit over adjacent feet (Fig. 10, *A* and *B*). However, while simple steric hindrance might contribute to the peculiar alternate disposition of tetrads over feet in the mature junction, it cannot by itself explain the development of this pattern. During formation of the junction, steric hindrance would prevent neither individual DHPRs from associating with adjacent feet (Fig. 10 *C*, *lower rows of feet*) nor the association of tetrads with feet at intervals >2:1 ratio (Fig. 10 *D*). Instead, we find that even when tetrads are incomplete, individual DHPRs occupy fixed positions in association with the subunits of alternate feet (Fig. 10 *C*, *top row of feet*). This means that even though DHPRs appear to associate with feet subunits individually and not in groups of four, they interact only with feet in odd positions of the array (1, 3, 5, etc.) and not with those in even positions (2, 4, 6, etc.). This striking exclusion of DHPR particles from half of the feet in the array suggests a molecular determination of the alternate association pattern. Since the large majority of RyRs in mouse muscle is of a single isoform (Takeshima et al., 1994; Giannini et al., 1995), it is unlikely that this pattern arises from a direct and preferential interaction of the DHPRs with a specific RyR isoform in that position (Block et al., 1996). Rather, we must assume that DHPRs assemble into tetrads in synchrony with the formation of feet arrays. This is also supported by the following consideration. If feet first formed extensive arrays and tetrads were acquired subsequently as a result of the infiltration of DHPRs into the junction from its periphery, the circular pattern shown in Fig. 10 *E* would develop. But subdomains with tetrads at the periphery, as opposed to the center, are not seen. Furthermore, subdomains of tetrads would then be expected to show the same orientation throughout a junction. The observation of multiple subdomains of tetrad arrays and feet with different orientations is more consistent with a concomitant radial growth of both arrays, starting from multiple seed points (Fig. 10 *F*). A simultaneous assembly of the arrays of feet and tetrads is also consistent with the joint emergence and early association of the two proteins shown by immunolabeling of rat primary cultures (Flucher et al., 1994) and BC_3H1 cells (present study).

DHPRs do not require the presence of RyRs for their insertion into peripheral couplings (Protasi, F., C. Fran-

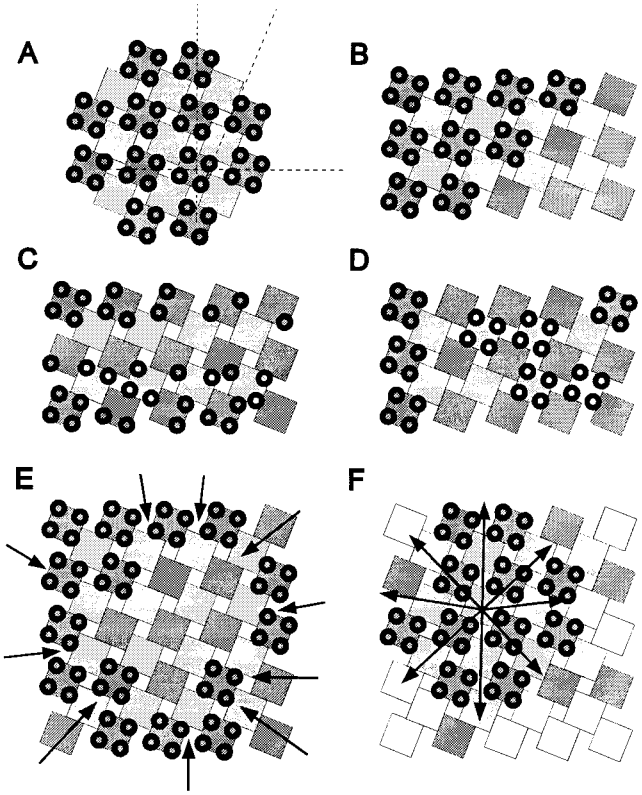

Figure 10. Formation of tetrad arrays in calcium release units. (*A*) Superimposed arrays of feet (*squares*) and tetrads (*groups of four circles*) represent the regular association of tetrads with every other foot. To emphasize this arrangement, adjacent rows of feet are drawn in different shades of gray. Dashed lines in *A* show the axes of the orthogonal array and the skew of the orientation of tetrads. Since the size of a tetrad is slightly larger than that of a foot, the association of tetrads with alternate feet (*B*) represents the densest packing possible. However, steric hindrance alone would not prevent either the positioning of tetrads at larger intervals (*D*) or the association of incomplete tetrads with neighboring feet (*C*, *bottom*). Such patterns are not observed; rather, complete and incomplete tetrads are always associated with alternate feet (*C*, *top row*), suggesting that the alternating association is determined by other factors. Formation of extensive arrays of feet before the incorporation of tetrads by centripetal diffusion and subsequent immobilization of tetrads opposite feet should result in arrays with unoccupied centers (*E*) that are never seen. The observations of multiple microarrays of tetrads and feet with different orientations within the larger junctions and the alternate disposition of tetrads are more consistent with a concomitant centrifugal growth of both arrays (*F*).

zini-Armstrong, and P.D. Allen, unpublished observations). However, in the presence of RyRs, DHPRs associate preferentially with those parts of the junctions where the arrays of feet are present. This was first shown in cardiac muscle (Protasi et al., 1996) and has now been confirmed for junctions assembled by skeletal muscle proteins. At present, a direct link between DHPRs and RyRs is debated; therefore this preferred association of tetrads and feet with each other may depend on additional junctional proteins (Caswell et al., 1991; Marty et al., 1994; Guo and Campbell, 1995). Immunolabeling of triadin shows that this protein, which has been implicated in the RyR–DHPR interaction, is expressed and inserted into the junction during the critical period.

Our findings emphasize the close spatial, and probably also temporal, relationship in the gradual assembly of the corresponding arrays of feet and tetrads within preformed SR–plasma membrane junctions. The strict adherence of DHPR particles to positions of alternate feet even during early stages of junction formation suggests a framework of conditions for the molecular organization of the e–c coupling apparatus in skeletal muscle that goes beyond simple steric hindrance dictated by the position of DHPRs relative to RyR subunits.

We thank Drs. A.H. Caswell, S. Fleischer, and S. Froehner for their generous gift of antibodies. This work was supported in part by National Institutes of Health grant 15835 to C. Franzini-Armstrong and the Pennsylvania Muscle Institute (CFA) and by grants from the Austrian National Bank (5353) and from the Fonds zur Förderung der wissenschaflichen Forschung (S06612-MED) to B.E. Flucher. B.E. Flucher is an Austrian Programme for Advanced Research and Technology fellow of the Austrian Academy of Sciences.

References

Adams, B.A., T. Tanabe, A. Mikami, S. Numa, and K.G. Beam. 1990. Intramembrane charge movement restored in dysgenic skeletal muscle by injection of dihydropyridine receptor cDNAs. *Nature (Lond.).* 346:569–572.

Airey, J.A., M.D. Baring, and J.L. Sutko. 1991. Ryanodine receptor protein is expressed during differentiation in muscle cell lines BC_3H1 and C2C12. *Dev. Biol.* 148:365–374.

Block, B.A., T. Imagawa, K.P. Campbell, and C. Franzini-Armstrong. 1988. Structural evidence for direct interaction between the molecular components of the transverse tubule/sarcoplasmic reticulum junction in skeletal muscle. *J. Cell Biol.* 107:2587–2600.

Block, B.A., J. O'Brien, and J. Franck. 1996. The role of ryanodine receptor isoforms in the structure and function of the vertebrate triad. *In* Organellar Ion Channels and Transporters. D.E. Clapham and B.E. Ehrlich, editors. The Rockefeller University Press, New York. 47–65.

Brandt, N.R., A.H. Caswell, S.-N. Wen, and J.A. Talvenheimo. 1990. Molecular interactions of the junctional foot protein and dihydropyridine receptor in skeletal muscle triads. *J. Membr. Biol.* 113:237–251.

Caffrey, J.M., and M.C. Farach. 1988. A monoclonal antibody specifically modulates dihydropyridine sensitive calcium current in BC_3H1 myocytes. *Mol. Pharmacol.* 34:518–526.

Caffrey, J.M., A.M. Brown, and M.D. Schneider. 1987. Mitogens and oncogenes can block the induction of specific voltage-gated ion channels. *Science (Wash. DC).* 236:570–573.

Caswell, A.H., N.R. Brandt, J.P. Brunschwig, and S. Purkerson. 1991. Localization and partial characterization of the oligomeric disulfide-linked molecular weight 95,000 protein (triadin) which binds the ryanodine and dihydropyridine receptors in skeletal muscle triadic vesicles. *Biochemistry.* 30:7507–7513.

Coronado, R., J. Morrissette, M. Sukhareva, and D.M. Vaughan. 1994. Structure and function of ryanodine receptors. *Am. J. Physiol.* 266:C1485–C1491.

Fan, H., N.R. Brandt, M. Peng, A. Schwartz, and A.H. Caswell. 1995*a.* Binding sites of monoclonal antibodies and dihydropyridine receptor α_1 subunit cytoplasmic II-III loop on skeletal muscle triadin fusion peptides. *Biochemistry.* 34:14893–14901.

Fan, H., N.R. Brandt, and A.H. Caswell. 1995*b.* Disulfide bonds, N-glycosylation and transmembrane topology of skeletal muscle triadin. *Biochemistry.* 34:14902–14908.

Flucher, B.E. 1992. Structural analysis of muscle development: transverse tubules, sarcoplasmic reticulum, and the triad. *Dev. Biol.* 154:245–260.

Flucher, B.E., and C. Franzini-Armstrong. 1996. Formation of junctions involved in excitation-contraction coupling in skeletal and cardiac muscle. *Proc. Natl. Acad. Sci. USA.* 93:8101–8106.

Flucher, B.E., M.E. Morton, S.C. Froehner, and M.P. Daniels. 1990. Localization of the α_1 and α_2 subunits of the dihydropyridine receptor and ankyrin in skeletal muscle triads. *Neuron.* 5:339–351.

Flucher, B.E., M. Terasaki, H. Chin, T. Beeler, and M.P. Daniels. 1991. Biogenesis of transverse tubules in skeletal muscle in vitro. *Dev. Biol.* 145:77–90.

Flucher, B.E., J.L. Phillips, J.A. Powell, S.B. Andrews, and M.P. Daniels. 1992. Coordinated development of myofibrils, sarcoplasmic reticulum and transverse tubules in normal and dysgenic mouse skeletal muscle, *in vivo* and *in vitro. Dev. Biol.* 150:266–280.

Flucher, B.E., H. Takekura, and C. Franzini-Armstrong. 1993*a.* Development of the excitation-contraction coupling apparatus in skeletal muscle: association of sarcoplasmic reticulum and transverse tubules with myofibrils. *Dev.*

Biol. 160:135–147.

Flucher, B.E., S.B. Andrews, S. Fleisher, A.R. Marks, A.H. Caswell, and J.A. Powell. 1993*b*. Triad formation: organization and function of the sarcoplasmic reticulum calcium release channel and triadin in normal and dysgenic muscle in vitro. *J. Cell Biol.* 123:1161–1174.

Flucher, B.E., S.B. Andrews, and M.P. Daniels. 1994. Molecular organization of transverse tubule/sarcoplasmic reticulum junctions during development of excitation-contraction coupling in skeletal muscle. *Molec. Biol. Cell.* 5:1105–1118.

Franzini-Armstrong, C. 1970. Studies of the triad. *J. Cell Biol.* 47:488–499.

Franzini-Armstrong, C., and A.O. Jorgensen. 1994. Structure and development of e-c coupling units in skeletal muscle. *Annu. Rev. Physiol.* 56:509–534.

Franzini-Armstrong, C., and J.W. Kish. 1995. Alternate disposition of tetrads in peripheral couplings of skeletal muscle. *J. Muscle Res. Cell Motil.* 16:319–324.

Franzini-Armstrong, C., M. Pincon-Raymond, and F. Rieger. 1991. Muscle fibers from dysgenic mouse in vivo lack a surface component of peripheral couplings. *Dev. Biol.* 146:364–376.

Giannini, G., A. Conti, S. Mammarella, M. Scrobogna, and V. Sorrentino. 1995. The ryanodine receptor/calcium channel genes are widely and differentially expressed in murine brain and peripheral tissues. *J. Cell Biol.* 128:893–904.

Guo, W., and K.P. Campbell. 1995. Association of triadin with the ryanodine receptor and calsequestrin in the lumen of sarcoplasmic reticulum. *J. Biol. Chem.* 270:9027–9030.

Holtzer, H.H., H. Holtzer, T. Hijikata, Z.H. Lin, Z.Q. Zhang, S. Holtzer, F. Protasi, C. Franzini-Armstrong, and H.L. Sweeney. 1997. Independent assembly of 1.6 μm long bipolar MHC filaments and I-Z-I bodies. *Cell Struct. Funct.* In press.

Ikemoto, N., M. Ronjat, G.L. Meszaris, and M. Koshita. 1989. Postulated role of calsequestrin in the regulation of calcium release from sarcoplasmic reticulum. *Biochemistry.* 28:6764–6771.

Imagawa, T., J.S. Smith, R. Coronado, and K.P. Campbell. 1987. Purified ryanodine receptor from skeletal muscle sarcoplasmic reticulum is the Ca^{2+}-permeable pore of the calcium release channel. *J. Biol. Chem.* 262:16636–16643.

Inui, M., A. Saito, and S. Fleischer. 1987. Purification of the ryanodine receptor and identity with feet structures of junctional terminal cisternae of sarcoplasmic reticulum from fast skeletal muscle. *J. Biol. Chem.* 262:1740–1747.

Jorgensen, A.O., A.C.-Y. Shen, W. Arnold, A.T. Leung, and K.P. Campbell. 1989. Subcellular distribution of the 1,4-dihydropyridine receptor in rabbit skeletal muscle in situ: an immunofluorescence and immunocolloidal gold-labeling study. *J. Cell Biol.* 109:135–147.

Kim, K.C., A.H. Caswell, J.A. Talvenheimo, and N.R. Brandt. 1990. Isolation of a terminal cisterna protein which may link the dihydropyridine receptor to the junctional foot protein in skeletal muscle. *Biochemistry.* 29:9281–9289.

Knudson, C.M., K.K. Stang, A.O. Jorgensen, and K.P. Campbell. 1993*a*. Biochemical characterization and ultrastructural localization of a major junctional sarcoplasmic reticulum glycoprotein (triadin). *J. Biol. Chem.* 268: 12637–12645.

Knudson, C.M., K.K. Stang, C.R. Moomaw, C.A. Slaughter, and K.P. Campbell. 1993*b*. Primary structure and topological analysis of a skeletal muscle-specific junctional sarcoplasmic reticulum glycoprotein (triadin). *J. Biol. Chem.* 268:12646–12654.

Lai, F.A., H.P. Erickson, E. Rousseau, Q.Y. Liu, and G. Meissner. 1988. Purification and reconstitution of the calcium release channel from skeletal muscle. *Nature (Lond.).* 331:315–319.

MacLennan, D.H., K.P. Campbell, and R.A.F. Reithmeier. 1983. Calsequestrin. *In* Calcium and Cell Function. 4:151–173.

Marks, A.R., P. Tempst, K.S. Hwang, M.B. Taubman, M. Inui, C. Chadwick, S. Fleisher, and B. Nadal-Girard. 1989. Molecular cloning and characterization of the ryanodine receptor/junctional channel complex cDNA from skeletal muscle sarcoplasmic reticulum. *Proc. Natl. Acad. Sci. USA.* 86:8683–8687.

Marks, A.R., M.B. Taubman, A. Saito, Y. Dai, and S. Fleisher. 1991. The ryanodine receptor/junctional channel complex is regulated by growth factors in a myogenic cell line. *J. Cell Biol.* 114:303–312.

Marty, I., M. Robert, M. Villaz, K. De Jongh, Y. Lai, W.A. Catteral, and M. Ronjat. 1994. Biochemical evidence for a complex involving dihydropyridine receptor and ryanodine receptor in triad junctions of skeletal muscle. *Proc. Natl. Acad. Sci. USA.* 91:2270–2274.

Meissner, G. 1975. Isolation and characterization of two types of sarcoplasmic reticulum vesicles. *Biochim. Biophys. Acta.* 389:51–68.

Meissner, G. 1994. Ryanodine receptor/Ca^{2+} release channels and their regulation by endogenous effectors. *Annu. Rev. Physiol.* 56:485–508.

Morton, M.E., and S.C. Froehner. 1987. Monoclonal antibody identifies a 200-kD α subunit of the dihydropyridine-sensitive calcium channel. *J. Cell Biol.* 262:11904–11907.

Morton, M.E., and S.C. Froehner. 1989. The α_1 and α_2 polypeptides of the dihydropyridine-sensitive calcium channel differ in developmental expression and tissue distribution. *Neuron.* 2:1499–1506.

Morton, M.E., J.M. Caffrey, A.M. Brown, and S.C. Froehner. 1988. Monoclonal antibody to the alpha 1-subunit of the dihydropyridine-binding complex inhibits calcium currents in BC_3H1 cells. *J. Biol. Chem.* 263:613–616.

Osame, M., A.G. Engel, C.J. Rebouche, and R.E. Scott. 1981. Freeze-fracture electron microscopic analysis of plasma membranes of cultured muscle cells in Duchenne dystrophy. *Neurology.* 31:972–979.

Pincon-Raymond, M., F. Rieger, M. Fosset, and M. Lazdunski. 1985. Abnormal transverse tubule system and abnormal amount of receptors for Ca^{2+} channel inhibitors of the dihydropyridine family in skeletal muscle from mice with embryonic muscular dysgenesis. *Nature (Lond.).* 325:717–720.

Pozzan, T., R. Rizzuto, P. Volpe, and J. Meldolesi. 1994. Molecular and cellular physiology of intracellular calcium stores. *Physiol. Rev.* 74:595–636.

Powell, J.A., L. Petherbridge, and B.E. Flucher. 1996. Formation of triads without the dihydropyridine receptor α subunits in cell lines from dysgenic skeletal muscle. *J. Cell Biol.* 134:375–387.

Protasi, F., X.-H. Sun, and C. Franzini-Armstrong. 1996. Formation and maturation of calcium release apparatus in developing and adult avian myocardium. *Dev. Biol.* 173:265–278.

Radermacher, M., V. Rao, R. Grassucci, J. Frank, A.P. Timerman, S. Fleisher, and T. Wagenknecht. 1994. Cryo-electron microscopy and three-dimensional reconstruction of the calcium release channel/ryanodine receptor from skeletal muscle. *J. Cell Biol.* 127:411–423.

Rampe, D., J.M. Caffrey, M.D. Schneider, and A.M. Brown. 1988. Control of expression of the 1-4 dihydropyridine receptor in BC_3H1 cells. *Biochem. Biophys. Res. Comm.* 152:769–775.

Rios, E., and G. Brum. 1987. Involvement of dihydropyridine receptors in excitation-contraction coupling in skeletal muscle. *Nature (Lond.).* 325:717–720.

Rios, E., J. Ma, and A. Gonzales. 1991. The mechanical hypothesis of excitation contraction coupling. *J. Muscle Res. Cell Motil.* 12:127–135.

Schneider, M.F. 1981. Membrane charge movements and depolarization-contraction coupling. *Annu. Rev. Physiol.* 43:507–517.

Schneider, M.F., and W.K. Chandler. 1973. Voltage dependence charge movement in skeletal muscle: a possible step in excitation contraction coupling. *Nature (Lond.).* 242:244–246.

Schubert, D., A.J. Harris, C.E. Devine, and S. Heinemann. 1974. Characterization of a unique muscle cell line. *J. Cell Biol.* 61:398–413.

Sorrentino, V., and P. Volpe. 1993. Ryanodine receptors: how many, where and why? *TIPS (Trends Pharmacol. Sci.).* 14:98–105.

Sun, X.-H., F. Protasi, M. Takahashi, H. Takeshima, D.G. Ferguson, and C. Franzini-Armstrong. 1995. Molecular architecture of membranes involved in excitation–contraction coupling of cardiac muscle. *J. Cell Biol.* 129:659–671.

Takekura, H., L. Bennet, T. Tanabe, K.G. Beam, and C. Franzini-Armstrong. 1994*a*. Restoration of junctional tetrads in dysgenic myotubes by dihydropyridine receptor cDNA. *Biophys. J.* 67:793–804.

Takekura, H., X.-H. Sun, and C. Franzini-Armstrong. 1994*b*. Development of the excitation-contraction coupling apparatus in skeletal muscle. Peripheral and internal calcium release units are formed sequentially. *J. Muscle Res. Cell Motil.* 15:102–118.

Takekura, H., H. Takeshima, S. Nishimura, M. Takahashi, T. Tanabe, V. Flockerzi, F. Hoffman, and C. Franzini-Armstrong. 1995. Co-expression in CHO cells of two muscle proteins involved in e-c coupling. *J. Muscle Res. Cell Motil.* 16:465–480.

Takeshima, H., M. Iino, H. Takekura, M. Nishi, J. Kuno, O. Minowa, H. Takano, and T. Noda. 1994. Excitation-contraction uncoupling and muscular degeneration in mice lacking functional skeletal muscle ryanodine-receptor gene. *Nature (Lond.).* 369:556–559.

Tanabe, T., K.G. Beam, J.A. Powell, and S. Numa. 1988. Restoration of excitation-contraction coupling and slow calcium current in dysgenic muscle by dihydropyridine receptor complementary DNA. *Nature (Lond.).* 336:134–139.

Taubman, M.B., C.W.J. Smith, S. Izumo, J.W. Grant, T. Endo, A. Andreadis, and B. Nadal-Ginard. 1989. The expression of sarcomeric muscle-specific contractile protein genes in BC_3H1 cells: BC_3H1 cells resemble skeletal myoblasts that are defective for commitment to terminal differentiation. *J. Cell Biol.* 108:1799–1806.

Yuan, S., W. Arnold, and A.O. Jorgensen. 1991. Biogenesis of transverse tubules and triads: immunolocalization of the 1,4-dihydropyridine receptor, TS28, and the ryanodine receptor in rabbit skeletal muscle developing in situ. *J. Cell Biol.* 112:289–301.